

# Indications for Nonbiological Reconstruction of Posttraumatic Bone Defects About the Knee

Kevin D. Tetsworth, MD, FAAOS, FRACS, FAOrthA,<sup>a,b,c</sup>  
Zhenya H. Welyczko, MBBS, FRACS, FAOrthA,<sup>a,d</sup> and Stephen M. Quinlan, MD, FAAOS<sup>e</sup>

**Summary:** 3D printing and modeling has continued to grow in popularity over the past decade because the technology has matured and become more affordable and widely available. The main indications for nonbiological reconstruction of large bone defects are principally those patients where the candidate is unlikely to be successful if reconstructed by other means. Bespoke, custom, patient-specific implants can be designed to very effectively address bone loss, incorporating design elements that are particular to the needs of any given unique clinical condition. These implants are generally designed as titanium scaffolds that encourage bony incorporation at the host implant junction both proximal and distal. These scaffolds are typically considered a cellular solid, with high porosity that also promotes bone ingrowth directly into the substance of the body of the implant. Titanium scaffolds of this type have become a useful treatment alternative for large segmental bone defects around the knee, especially distal femoral defects. These are often adult patients with local or systemic compromise, or instead they may be too young to be considered candidates for reconstruction using a megaprosthesis. The process requires careful evaluation of individual patients, then matching that patient with the best treatment option, while recognizing the expectations and demands specific to that particular patient. Several cases are presented here to illustrate the variety of indications that can be successfully addressed with this technology, highlighting the quality of the clinical outcome that can be achieved despite the complexity of the pathology encountered.

**KEY WORDS:** limb reconstruction, bone loss, bone defect, 3D printing, custom scaffolds, patient-specific implants, orthopaedic surgery

(*J Orthop Trauma* 2024;38:S23–S29)

## INTRODUCTION

Since the advent of 3D printing in the 1980s, its popularity has grown tremendously, and as this technology has gradually become more accessible and affordable over the past decade, it is now considered essentially mainstream throughout medicine.<sup>1–3</sup> Nowhere is this more obvious than in orthopaedic surgery, and the routine clinical practice of most surgeons already incorporates many aspects of 3D modeling and virtual procedures on a daily basis.<sup>1–3</sup> Many implants are now designed and produced based on 3D models generated as idealized realizations of local anatomy.<sup>4,5</sup> Several manufacturers have emerged that are dedicated to providing custom arthroplasty components, titanium scaffolds, and other orthopaedic implants tailored to the specific details of the unique anatomy of an individual patient. Perhaps more importantly, hundreds of procedures are conducted daily where 3D modeling and virtual surgery have become an integral part of the actual procedure. 3D modeling has of course become standard practice in many operating theaters, typically in the form of virtual surgical procedures for preoperative planning<sup>3,6–9</sup> or intraoperatively through navigation.<sup>3,10–13</sup> Our assumption is that 3D printing and modeling now plays an important role in many of the more complex orthopaedic cases currently treated around the world. This is most evident in the realm of adult reconstructive surgery<sup>7,12</sup> and joint arthroplasty<sup>3,13–16</sup> but has now essentially permeated every aspect of orthopaedic surgery, including trauma,<sup>4,8,17–20</sup> spine,<sup>21,22</sup> hand,<sup>8,20,23</sup> shoulder,<sup>6,9</sup> tumor,<sup>5,24</sup> and sports medicine.<sup>9</sup>

This review describes and illustrates several cases where patient-specific 3D-printed titanium scaffolds were used.<sup>18,25,26</sup> The processes involved in creating the implant and the important elements to consider when addressing a specific surgical situation have been described in depth in earlier publications.<sup>18,25,26</sup> These particular cases have been selected to demonstrate the variety of indications that are encountered and can be successfully addressed with this technology, while highlighting the quality of the clinical outcome that can be achieved despite the complexity of the pathology. The cases also briefly allude to the nature of the process involved from start to finish, while focusing on the treatment options and rationale for choosing a custom 3D-printed titanium scaffold

Accepted for publication January 5, 2024.

From the <sup>a</sup>Department of Orthopaedic Surgery, The Royal Brisbane and Women's Hospital, Brisbane, Australia; <sup>b</sup>Orthopaedic Research Centre of Australia, Brisbane, Australia; <sup>c</sup>Herston Biofabrication Institute, Brisbane, Australia; <sup>d</sup>Department of Orthopaedic Surgery, The Princess Alexandra Hospital, Brisbane, Australia; and <sup>e</sup>The Paley Orthopedic and Spine Institute, St. Mary's Medical Center, West Palm Beach, FL.

K. D. Tetsworth reports no conflicts of interest declared related to this manuscript; consultant and speaker's bureau—Smith and Nephew, AO Foundation, OrthoDx, and BioBKN. Z. H. Welyczko reports no conflicts of interest declared related to this manuscript; no other conflicts to declare. S. M. Quinlan reports no conflicts of interest declared related to this manuscript; consultant Smith and Nephew, Globus Medical, NuVasive Specialized Orthopedics, OsteoCentric, Stryker, AO Foundation, Bone Support, Biocomposites, and EDGE Medical.

Reprints: Kevin D. Tetsworth, Department of Orthopaedic Surgery, Royal Brisbane and Women's Hospital Level 7, Ned Hanlon Building, Butterfield St, Herston, QLD, Australia 4029 (e-mail: kevin.tetsworth@health.qld.gov.au).

Copyright © 2024 Wolters Kluwer Health, Inc. All rights reserved.

DOI: 10.1097/BOT.0000000000002764

and some of the important implant design considerations specific to each case.

## INDICATIONS

The main indications for nonbiological reconstruction of large segmental bone loss are principally those patients where the candidate is unlikely to be successful if reconstructed by other means.<sup>27–29</sup> Other treatment alternatives include the Masquelet-induced membrane technique,<sup>30,31</sup> distraction osteogenesis (Ilizarov methods or externally controlled/powered telescopic nails),<sup>32–35</sup> vascularized free-tissue transfers,<sup>36</sup> more conventional megaprosthesis/arthroplasty,<sup>37</sup> or amputation with/without osseointegration.<sup>38,39</sup> A small subset of selected patients are better suited for alternative, nonbiological reconstructions of posttraumatic bone defects about the knee, most often using a custom designed patient-specific 3D-printed implant.

Many patients are simply physiologically unsuitable for biological reconstructive options, including both the Masquelet technique<sup>30,31</sup> and Ilizarov methods (distraction osteogenesis).<sup>32–35</sup> These patients are generally severely immunocompromised and may have chronic renal failure, diabetes mellitus, hepatic insufficiency, or AIDS.<sup>40</sup> Many of these patients would have difficulty regenerating new bone, or the healing response may be so limited that bone grafts fail to incorporate.<sup>27–29</sup> Alternatively, other patients may not be suitable for these procedures because of balance or mobility issues that would limit their ability to complete either a staged reconstruction or a protracted treatment protocol. This would include patients with Parkinson disease, blindness, or multiple sclerosis or where the contralateral lower limb has been amputated. These are patients who require a more aggressive solution to restore mobility by allowing almost immediate weight-bearing. Other patients may be unsuitable because they have cognitive issues, such as dementia or autism, or have psychiatric issues that preclude their ability to cooperate in either a staged reconstruction or a protracted treatment protocol. Finally, some patients, by their age alone, are considered unattractive candidates. The truly young patients, younger than 40 years, are more often excluded from many arthroplasty procedures involving the knee and are therefore subjected to more prolonged reconstructive efforts, such as methods involving distraction osteogenesis. Older patients, older than 65 years, are more likely to be considered very good candidates for conventional arthroplasty options, even if it requires a megaprosthesis. However, there are those patients who reside between young and old, where arthroplasty is less attractive and who are also less likely to successfully complete reconstruction through biological methods.

### Case 1

The first case involves a 51F paramedic who sustained a type I open right distal femur fracture with a 1-cm puncture wound medially after falling from a bicycle (Fig. 1). The patient underwent an open reduction internal fixation (ORIF) through a lateral approach with a lateral locked plate at a peripheral hospital. The medial puncture wound was not opened or explored. The patient presented 7 weeks later with

a fever, rigors, and a draining sinus through the lateral scar, and the fracture had not yet united. The patient underwent open lavage and debridement with a vacuum dressing on 3 occasions at the peripheral hospital. Cultures grew *Mycobacterium fortuitum*, and the patient was subsequently referred to our tertiary center for further treatment. The medial wound at this time was completely benign clinically.

The patient underwent further debridement, with removal of implants and revision ORIF with insertion of an antibiotic plate and beads through the lateral approach. The lateral cortex had a 25 × 40-mm area of devitalized bone underneath the plate, which was excised, with a 29 cm<sup>3</sup> bone defect after debridement. This wound closed easily but had persistent drainage; a second debridement was completed, and another revision ORIF was performed. Further devitalized bone was debrided, and the remaining now segmental defect measured 86 mm/46 cm<sup>3</sup>. An antibiotic PMMA spacer was used to fill the defect, and cultures again grew *Mycobacterium fortuitum*. Because of the persistent drainage, the patient underwent a third debridement, and this time, the previous medial open wound was incorporated in the exposure. All implants, spacers, and biofilm were removed, and revision ORIF with another Ab-PMMA spacer was performed, including a medial plate. Cultures now grew *Mycobacterium fortuitum* and *Candida parapsilosis*. After this procedure, including open medial debridement as well, the wound healed uneventfully, and they received a course of systemic antibiotic treatment for both microorganisms. Serum markers returned to normal, and the infection seemed to have been clinically eradicated.

Computed tomography (CT) scans of both the femurs were performed to plan for a 3D-printed custom titanium scaffold. Distal femur replacement with a megaprosthesis was considered, but given the patient's young age, high levels of expected activity, and intact articular surfaces, the decision was made to perform reconstruction with preservation of the native joint.

The second stage reconstruction was performed 4 months after the final debridement/first stage procedure. The patient-specific custom titanium scaffold was designed with a hemispherical extension distally into the remaining metaphyseal cancellous bone to increase surface contact and to resist shear and translation. When inserted, a small acetabular reamer was used to create the concavity for this in the metaphysis. An exterior skin of highly polished titanium was incorporated into the design to replace an area of destroyed trochlear surface and to allow the patella to articulate with a smooth surface rather than the scaffold. The proximal end of the implant also had a crown extension that extends into the medullary canal, to further stabilize the implant by eliminating translation. The medial plate was left in situ, and a new lateral plate was applied that provided more anatomic fit, based on 3D modeling. The modeling had revealed that the patient had a proximal bow to their femur that would not allow a longer lateral plate, and a 9-hole plate was used to allow the plate to conform most closely. The reamer-irrigator-aspirator was used to harvest autologous graft from the contralateral femoral canal, mixed with cancellous allograft chips to increase the volume. The induced membrane that

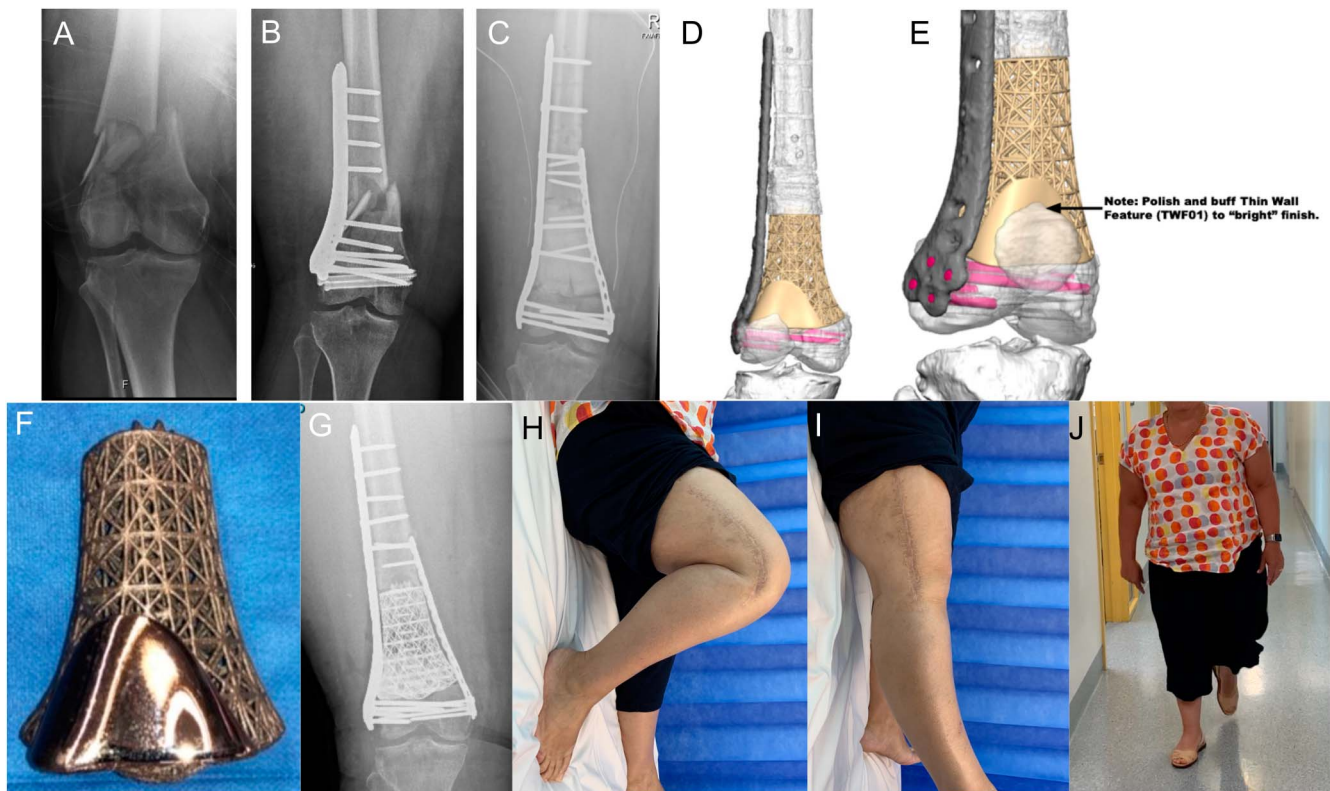


**FIGURE 1.** A 51F sustained a type 1 open comminuted right T-intercondylar distal femur fracture in a fall from a bicycle; A, initial AP radiograph; B, AP radiograph of the primary internal fixation with a lateral locked plate; C, this became infected within 7 weeks, and the patient was then referred for tertiary care. They underwent a series of open debridements, culminating in revision ORIF with dual plates and including a PMMA antibiotic spacer; D, 3D model of the CT scan of the construct and bone defect, designing a patient-specific titanium scaffold to fill the void; E, detailed view of the custom titanium scaffold, incorporating a polished thin wall coating the area intended to recreate the patellofemoral articulating surface; F, the custom implant, highlighting the polished external surface for articulation with the patella; G, AP radiograph at 1-year postoperative, with no evidence of loosening of the implant; H, I, clinical images 18 months postoperative demonstrating the range of motion of the adjacent right knee, including 115 degrees flexion, full extension, and no extensor lag; J, clinical image during gait, confirming the patient is able to fully weight-bear on the limb. AP, anteroposterior.

developed during the interim between stages was preserved, and the bone surfaces freshened with minor cuts as planned preoperatively in a virtual procedure. A femoral distractor was used to open up the space to allow insertion of the scaffold; this was filled with graft immediately before the insertion, concentrating most of the grafts at the proximal and distal ends of the scaffold.

The patient was kept touch weight-bearing only for 6 weeks but allowed full range of motion immediately. The wound again healed uneventfully, and 18 months later, they continue to do extremely well with normal serum markers. The patient has minimal pain with a range of motion of 0–115 degrees with no extensor lag, walks full weight-bearing unaided, and has returned to cycling and other activities without restriction.

## Case 2

The second case involves a 73F insulin-dependent diabetic (IDDM) who fell several feet from a step ladder and

sustained a closed comminuted T-intercondylar left distal femur fracture (Fig. 2). The patient underwent ORIF with a lateral locked distal femoral plate as a bridging construct through a less invasive approach. This quickly became infected, and when it failed to respond to open debridement and antibiotic beads, they were referred for limb salvage versus amputation. The patient was managed in a staged fashion with open debridement, and the first stage consisted of removal of all former implants, subsegmental resection of 10.3 cm of distal femoral metadiaphysis, insertion of a solid polymethylmethacrylate (PMMA) antibiotic spacer, and revision ORIF.

This could have been converted to a distal femur replacement with a hinged arthroplasty design, but the knee joint was radiographically pristine despite their relatively advanced age. Preserving the joint required design and manufacture of a patient-specific 3D-printed custom titanium scaffold to completely fill the bone defect. This was an early design, and the implant itself was designed to

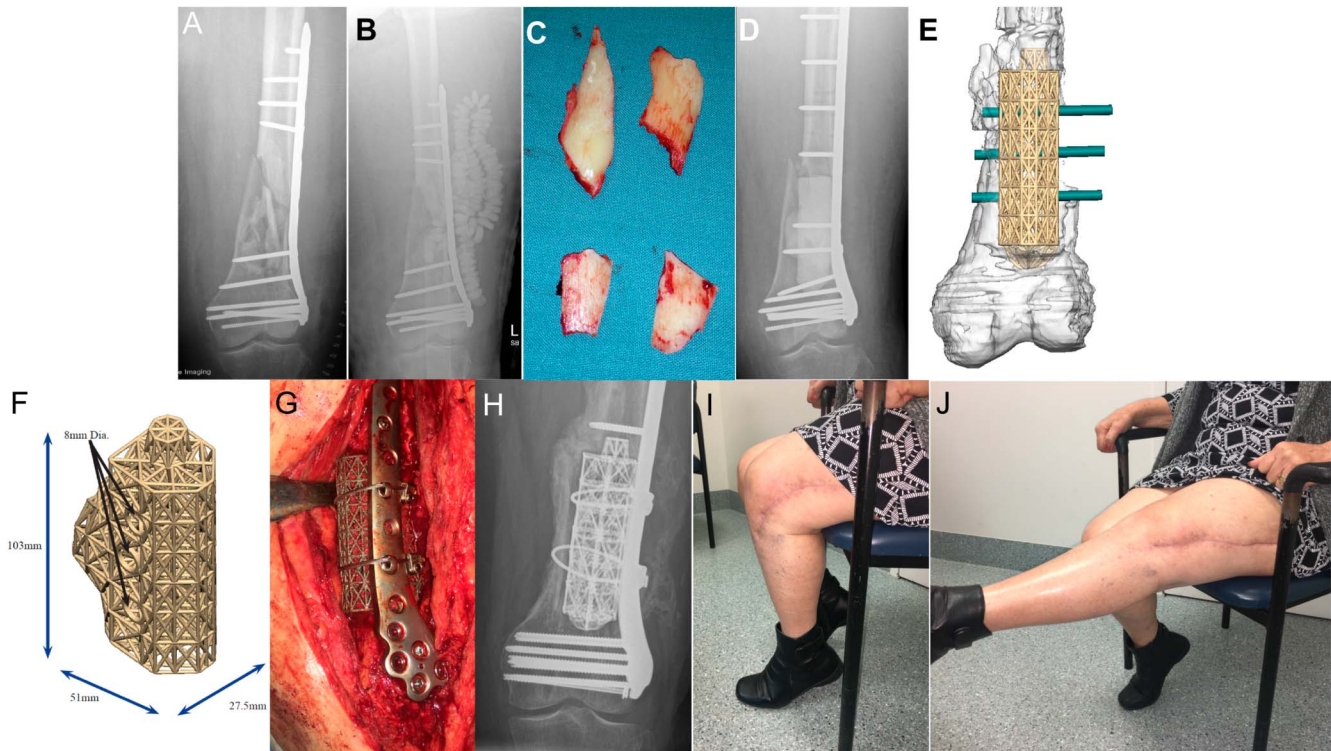


**FIGURE 2.** A 73F IDDM sustained a closed comminuted left extra-articular distal femur fracture in a fall from a step ladder; A, AP radiograph of the primary fixation using a lateral locked plate; B, subsequent AP radiograph after this became infected and failed to respond to repeated debridement and Ab-PMMA beads; C, the patient was referred for possible amputation, and during further debridement multiple devitalized bone fragments were removed; D, AP radiograph after revision ORIF with another lateral locked plate, and a solid PMMA spacer filling the defect; E, 3D model of the CT scan of the construct and defect, designing a patient-specific titanium scaffold to fill the void incorporating screw holes; F, detailed view of the custom titanium scaffold, replicating the size and shape of the PMMA spacer; G, intraoperative image of the scaffold inserted into the distal femur, with autogenous bone graft filling the scaffold; H, AP radiograph 3 months postoperative, with bone enveloping the scaffold and proceeding to solid union; I, J, clinical images >5 years postoperative demonstrating the range of motion of the adjacent knee, including 95 degrees flexion, full extension, and no extensor lag. AP, anteroposterior.

match the volume and contours of the PMMA spacer. Because this technology has matured, current designs instead now correspond very closely to the volume and contours of the missing bone, based on a bone modeled using the mirror image of the uninvolved contralateral limb as a template.

The second stage exchange was completed 15 weeks after the first stage (debridement and solid antibiotic polymethylmethacrylate [Ab-PMMA] spacer), with the custom titanium scaffold secured with a long lateral locked plate augmented with 2 cables. Autologous cancellous graft obtained using the reamer-irrigator-aspirator was applied liberally over the surface of the titanium scaffold. This implant was designed with a hemispherical extension distally into the remaining metaphyseal cancellous bone to increase the surface contact and resist shear and translation. Similarly, the proximal end of the implant has a crown extension of 8 mm that extends into the medullary canal of the diaphysis. This is again conducted to enhance the contact and limit shear/translation at the proximal host/implant junction. This is perhaps a more important design consideration for those

stabilized with an intramedullary nail, where the fixation is less rigid and residual motion is a greater risk.

The patient was allowed unrestricted motion immediately postoperative and instructed on partial weight-bearing (50%) for the first 12 weeks. When they returned in early follow-up at 3 months, it was clear that the patient had been ambulating full weight-bearing on the limb for many weeks prior because they walked in unsupported with a normal gait. The patient has continued to do extremely well and was recently seen 7 years postoperatively; they currently walk unaided in the community (80F), have minimal to no pain, and a range of motion from full extension to 95 degrees flexion.

### Case 3

The third case involves a 53F with a bipolar personality disorder who originally presented some years before with a 6.8-cm leg length discrepancy (LLD) after sustaining poly-trauma several years before, resulting in ORIF of the left acetabulum that later progressed with posttraumatic arthritis, and the patient had undergone a successful left total hip

replacement (Fig. 3). To address the considerable discrepancy, the right femur was lengthened with an intramedullary skeletal kinetic distractor nail, but psychiatric issues became more evident early postoperatively when the patient became noncompliant, and the regenerate bone subsequently failed to mature. This was salvaged with an intercalary allograft that several years later became infected and began to resorb and threatened to spread hematogenously to the contralateral hip arthroplasty. The patient was then managed in a staged

fashion with open debridement, and the first stage consisted of removal of the remaining allograft and all former implants, segmental resection of 14.2 cm of femoral diaphysis, insertion of a solid PMMA antibiotic spacer, and revision intramedullary (IM) nailing.

This could have been reconstructed through a staged bone grafting into a Masquelet-induced membrane, but the defect significantly exceeds 8 cm, and the risk of treatment failure is substantially increased. Alternatively, this could have

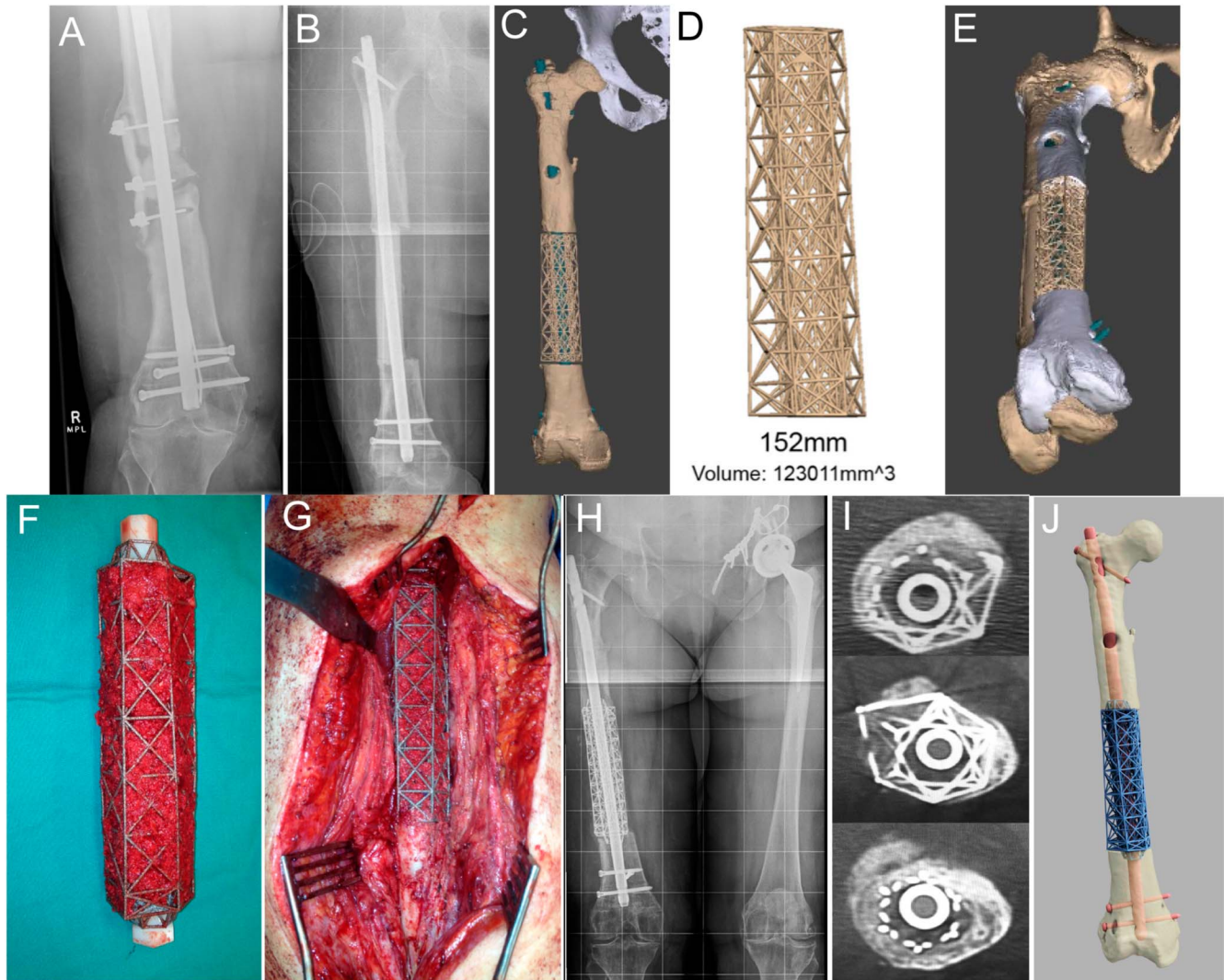


**FIGURE 3.** A 53F with a personality disorder who had undergone 6.8 cm lengthening of the right femur with a telescopic nail that failed to unite, and was salvaged with an intercalary allograft that several years later became infected; A, AP radiograph of the infected nonunion of the allograft in the right femoral diaphysis; B, AP radiograph after a 15 cm resection of the area involved, stabilized with an IM nail and a solid PMMA antibiotic spacer; C, 3D model of the CT scan of the construct and bone defect, designing a patient-specific titanium scaffold to fill the void; D, detailed view of the custom titanium scaffold; E, the virtual surgical procedure based on the 3D model with correction of a 19-degree external rotation deformity and 4 degrees of valgus (current position in gold; corrected position in white); F, autogenous bone graft filling the substance of the scaffold; G, intraoperative image of the scaffold inserted into the defect; H, AP radiograph of the construct 9 months postoperative, with solid ingrowth on each end of the implant; I, CT scan images at multiple levels at 9 months postoperative, confirming solid bone envelopes the implant; J, final modeled image of the reconstructed right femur, IM nail, and custom titanium scaffold. AP, anteroposterior.

been reconstructed using bone transport, but at that time, plate-assisted transport using telescopic nails had not yet been developed. Given her limited compliance with the original limb lengthening, she was considered incompatible with prolonged external fixation. A patient-specific 3D-printed custom titanium scaffold was instead manufactured to completely fill the defect, to limit the need for patient compliance and cooperation and allow the earliest possible return to unrestricted weight-bearing and activity. This implant reproduces the volume and contours of the original bone, as modeled using the mirror image of the uninvolved contralateral limb as a template.

The second stage exchange was completed 16 weeks after the first stage (debridement and solid Ab-PMMA spacer), with the custom titanium scaffold secured with an exchange to another IM nail. This was conducted primarily because this was more diaphyseal in nature and far more suitable to the load-sharing mechanics characteristic of intramedullary fixation. Autologous cancellous graft obtained using the reamer-irrigator-aspirator was applied liberally over the surface of the titanium scaffold. This implant was designed with a crown extension of 8 mm that extends into the medullary canal of the diaphysis on both ends of the implant. This is again conducted to enhance the contact and limit shear/translation at the host/implant junction. This is an extremely important design consideration for those scaffolds stabilized with an intramedullary nail, where the fixation is less rigid and residual motion is a greater risk.

The patient was allowed unrestricted motion immediately postoperative and instructed on partial weight-bearing (50%) for the first 12 weeks. When they returned in early follow-up at 3 months, the bone graft was already demonstrating radiographic early incorporation at both ends. This was confirmed with a CT scan at 4 months, with severe artefact from the titanium scaffold obscuring the extent of bone penetration into the body of the scaffold itself. One strut in the implant failed early, but with a scaffold of this type of design, the remaining intact individual struts (multiple) then absorb the additional stress. The patient has continued to do very well and was recently seen almost 8 years postoperatively; currently, they walk unaided in the community, with hip pain secondary to unrelated hip degenerative arthritis and a knee range of motion from full extension to 80 degrees flexion.

## DISCUSSION

Bespoke, patient-specific implants manufactured on demand using 3D printers have in our opinion opened new horizons within posttraumatic reconstruction. Contemporary surgeons are provided with an unprecedented capability to design and manufacture custom 3D-printed titanium scaffolds/implants to address the extremely difficult problem of segmental bone loss and correct other complex deformities.<sup>18,25,26</sup> Truss configurations are well-known in engineering to provide great strength with less mass.<sup>25,26</sup> These constructs are mechanically robust, with structural stability that facilitates immediate motion and early weight-bearing.<sup>18,25,26</sup> This architecture also acts as a lattice for bone graft and can be used in combination with the Masquelet-

induced membrane technique.<sup>18,25,26,30,31</sup> These implants are designed in a virtual surgical procedure that provides a patient-specific option for realignment and length correction.<sup>25</sup> The staged approach plays a critical role in the success of the procedure, and the membrane develops during an interim period between stages when the custom implant is first designed and then produced. The induced membrane creates a more favorable recipient bed for the reconstruction, producing growth factors that encourage more rapid incorporation of the graft.<sup>26,30,31</sup>

Reconstruction of a mangled, traumatized extremity by any means is almost always a long and arduous process for both surgeon and patient. For many of those involved in limb salvage, this difficult work has frequently required prolonged periods of external fixation and gradual correction through distraction osteogenesis. Unfortunately, these methods are characteristically prone to their own set of complications, including pin site infections, nonunions, scarring, and limitation of motion. Segmental bone loss further complicates attempts at reconstruction, and patients and surgeons in wealthier nations have benefited from a gradual transition toward methods that achieve distraction osteogenesis using externally controlled powered telescopic nails to achieve bone transport. The Masquelet-induced membrane technique is an attractive alternative in many environments, but the ideal parameters for timing and the source of bone graft remain problematic.<sup>26,30,31</sup> This method similarly has its own inherent limitations, and defects exceeding 8 cm in length are still at risk of complications and treatment failure.<sup>31</sup>

Bone defects about the knee continue to challenge orthopaedic surgeons, regardless of whether they are the result of a tumor, trauma, or infection.<sup>27–29</sup> A number of sophisticated techniques for the treatment of large skeletal defects have been developed over the past 50 years, including distraction osteogenesis,<sup>32–35</sup> the induced membrane technique,<sup>30,31</sup> vascularized bone transfer,<sup>36</sup> and 3D-printed patient-specific custom titanium scaffolds,<sup>18,25,26</sup> and each has their own advantages and disadvantages. Many of these alternatives are painful with high complication rates and have a genuine risk of treatment failure.<sup>27–29,38</sup> The complex efforts necessary to achieve union in these difficult cases inevitably results in a tremendous economic burden on the health care system, whereas the potential of ultimately requiring an amputation remains a very real possibility.<sup>27,38,39</sup> It is incumbent on the responsible surgeon to carefully evaluate individual patients and then match that patient with the best treatment option, recognizing the demands and expectations specific to that particular patient. Patient outcomes are ultimately dictated by the number of treatment options a surgeon can safely and effectively provide for any given circumstance; the more options available, the more likely one can be selected that best matches their needs.<sup>40</sup>

## REFERENCES

1. Tetsworth K, Mettyas T. Overview of emerging technology in orthopaedic surgery: what is the value in 3D modelling and printing? *Tech Orthop*. 2016;31:143–152.
2. Green N, Glatt V, Tetsworth K, et al. A practical guide to image processing in the creation of 3D models for orthopedics. *Tech Orthop*. 2016; 31:153–163.

3. Alemayehu DG, Zhang Z, Tahir E, et al. Preoperative planning using 3D printing technology in orthopedic surgery. *Biomed Res Int.* 2021;2021:7940242.
4. Buford WL, Jr, Turnbow BJ, Gugala Z, et al. Three-dimensional computed tomography-based modeling of sagittal cadaveric femoral bowing and implications for intramedullary nailing. *J Orthop Trauma.* 2014;28:10–16.
5. McCulloch RA, Frisoni T, Kurunskal V, et al. Computer navigation and 3D printing in the surgical management of bone sarcoma. *Cells.* 2021;10:195.
6. Iannotti JP, Weiner S, Rodriguez E, et al. Three-dimensional imaging and templating improve glenoid implant positioning. *J Bone Joint Surg Am.* 2015;97:651–658.
7. Jastifer JR, Gustafson PA. Three-dimensional printing and surgical simulation for preoperative planning of deformity correction in foot and ankle surgery. *J Foot Ankle Surg.* 2017;56:191–195.
8. Kataoka T, Oka K, Miyake J, et al. 3-Dimensional prebent plate fixation in corrective osteotomy of malunited upper extremity fractures using a real-sized plastic bone model prepared by preoperative computer simulation. *J Hand Surg Am.* 2013;38:909–919.
9. Sheth U, Theodoropoulos J, Abouali J. Use of 3-dimensional printing for preoperative planning in the treatment of recurrent anterior shoulder instability. *Arthrosc Tech.* 2015;4:e311–e316.
10. Hohmann E, Bryant A, Tetsworth K. A comparison between imageless navigated and manual freehand technique acetabular cup placement in total hip arthroplasty. *J Arthroplasty.* 2011;26:1078–1082.
11. Hohmann E, Bryant A, Tetsworth K. Accuracy of acetabular cup positioning using imageless navigation. *J Orthop Surg Res.* 2011;6:40.
12. Seon JK, Kim HS, Kim DY, et al. Navigation guided open wedge high tibial osteotomy. *J Korean Orthop Assoc.* 2014;49:107–117.
13. Siston R, Giori N, Goodman SB, et al. Surgical navigation for total knee arthroplasty: a perspective. *J Biomech.* 2007;40:728–735.
14. Krishnan SP, Dawood A, Richards R, et al. A review of rapid prototyped surgical guides for patient-specific total knee replacement. *J Bone Joint Surg Br.* 2012;94:1457–1461.
15. Nieminen J, Pakarinen T-K, Laitinen M. Orthopaedic reconstruction of complex pelvic bone defects. Evaluation of various treatment methods. *Scand J Surg.* 2013;102:36–41.
16. Sariali E, Boukhelifa N, Catonne Y, et al. Comparison of three-dimensional planning-assisted and conventional acetabular cup positioning in total hip arthroplasty. A randomized controlled trial. *J Bone Joint Surg Am.* 2016;98:108–116.
17. Geerling J, Kendoff D, Citak M, et al. Intraoperative 3D imaging in calcaneal fracture care. Clinical implications and decision-making. *J Trauma.* 2009;66:768–773.
18. Abar B, Kwon N, Allen NB, et al. Outcomes of surgical reconstruction using custom 3D-printed porous titanium implants for critical-sized bone defects of the foot and ankle. *Foot Ankle Int.* 2022;43:750–761.
19. Jeong H-S, Park K-J, Kil K-M, et al. Minimally invasive plate osteosynthesis using 3D printing for shaft fractures of clavicles: technical note. *Arch Orthop Trauma Surg.* 2014;134:1551–1555.
20. Leong N, Buijze GA, Fu EC, et al. Computer-assisted versus non-computer-assisted preoperative planning of corrective osteotomy for extra-articular distal radius malunions: a randomized controlled trial. *BMC Musculoskelet Disord.* 2010;11:282.
21. Anastasio AT, Peairs EM, Tabarestani TQ, et al. The expanding use of three dimensional printing in orthopaedic and spine surgery. *J Spine Surg.* 2022;8:300–303.
22. Cho W, Job AV, Chen J, et al. A review of current clinical applications of three-dimensional printing in spine surgery. *Asian Spine J.* 2018;12:171–177.
23. Miyake J, Murase T, Oka K, et al. Computer-assisted corrective osteotomy for malunited diaphyseal forearm fractures. *J Bone Joint Surg Am.* 2012;94:e150.
24. Handels H, Ehrhardt J, Plötz W, et al. Three-dimensional planning and simulation of hip operations and computer-assisted construction of endoprostheses in bone tumor surgery. *Comput Aided Surg.* 2001;6:65–76.
25. Tetsworth K, Block S, Glatt V. Putting 3D modelling and 3D printing into practice: virtual surgery and preoperative planning to reconstruct complex post-traumatic skeletal deformities and defects. *SICOT J.* 2017;3:16.
26. Tetsworth K, Woloszyk A, Glatt V. 3D printed titanium cages combined with the Masquelet technique for the reconstruction of segmental femoral defects: preliminary clinical results and molecular analysis of the biological activity of human-induced membranes. *OTA Int.* 2019;2:e016.
27. Pollak AN, Ficke JR, Extremity War Injuries III Session Moderators. Extremity war injuries: challenges in definitive reconstruction. *J Am Acad Orthop Surg.* 2008;16:628–634.
28. Maceroli MA, Gage MJ, Wise BT, et al. Risk factors for failure of bone grafting of tibia nonunions and segmental bone defects: a new preoperative risk assessment score. *J Orthop Trauma.* 2017;31(suppl 5):S55–S59.
29. Tetsworth KD, Burnand HG, Hohmann E, et al. Classification of bone defects: an extension of the orthopaedic trauma association open fracture classification. *J Orthop Trauma.* 2021;35:71–76.
30. Hoit G, Kain MS, Sparkman JW, et al. The induced membrane technique for bone defects: basic science, clinical evidence, and technical tips. *OTA Int.* 2021;4:e106.
31. Masquelet A, Kanakaris NK, Obert L, et al. Bone repair using the Masquelet technique. *J Bone Joint Surg Am.* 2019;101:1024–1036.
32. Papakostidis C, Bhandari M, Giannoudis PV. Distraction osteogenesis in the treatment of long bone defects of the lower limbs: effectiveness, complications and clinical results; a systematic review and meta-analysis. *Bone Joint J.* 2013;95-B:1673–1680.
33. Quinnan SM. Segmental bone loss reconstruction using ring fixation. *J Orthop Trauma.* 2017;31(suppl 5):S42–S46.
34. Quinnan SM. Use of a motorized intramedullary bone transport nail for trauma: tips, tricks, corticotomy techniques, and rate and rhythm. *J Orthop Trauma.* 2021;35(suppl 4):S31–S38.
35. Tetsworth K, Paley D, Sen C, et al. Bone transport versus acute shortening for the management of infected tibial non-unions with bone defects. *Injury.* 2017;48:2276–2284.
36. Beris AE, Lykissas MG, Korompilias AV, et al. Vascularized fibula transfer for lower limb reconstruction. *Microsurgery.* 2011;31:205–211.
37. Hoellwarth JS, Fourman MS, Crossett L, et al. Equivalent mortality and complication rates following periprosthetic distal femur fractures managed with either lateral locked plating or a distal femoral replacement. *Injury.* 2018;49:392–397.
38. MacKenzie EJ, Bosse MJ, Kellam JF, et al. Factors influencing the decision to amputate or reconstruct after high-energy lower extremity trauma. *J Trauma.* 2002;52:641–649.
39. Hoellwarth JS, Tetsworth K, Rozbruch SR, et al. Osseointegration for amputees: current implants, techniques, and future directions. *JBJS Rev.* 2020;8:e0043.
40. Tetsworth K, Cierny GC. Osteomyelitis debridement techniques. *Clin Orthop Relat Res.* 1999;360:87–96.